Temperature Coefficients in Compensated Silicon Solar Cells Investigated by Temperature Dependent Lifetime Measurements and Numerical Device Simulation

Halvard Haug[1, a)], Åsmund Skomeland[1], Rune Søndenå[1], Marie Syre Wiig[1], Charly Berthod[2] and Erik Stensrud Marstein[1]

[1]*Institute for Energy Technology, Instituttveien 18, 2007 Kjeller, Norway*
[2]*University of Agder, Jon Lilletunsvei 9, 4879 Grimstad, Norway,*

[a)]Corresponding author: halvard.haug@ife.no

Abstract. Silicon solar modules typically operate at a higher temperature than the 25 °C used for standard testing, and the temperature coefficient (TC) therefore might have a significant impact on the field performance. In this paper the temperature dependent behavior of compensated Si solar cells has been simulated using PC1Dmod6.2, using a combination of physical models which include the effect of both temperature and compensation doping. The simulations were based on experimental input measured on two high performance multicrystalline ingots of similar resistivity of ~1.3 Ωcm, as well as one ingot with a resistivity of 0.5 Ωcm. Two of the ingots are produced using Elkem Solar Silicon (ESS®), a compensated Si feedstock made using a metallurgical purification route, and the third is made from non-compensated reference material. Dopant concentrations as a function of height in the ingot were determined using a combination of experimental resistivity data, simulations and the Scheil equation. Temperature dependent lifetime images, measured on etched and passivated wafers after relevant solar cell processing steps were also acquired at different heights and used as input to the simulations. Taking all this into account, the simulated TC in the efficiency were found to be similar for the two 1.3 Ωcm ingots and slightly higher (less negative) in the 0.5 Ωcm ingot, mostly caused by differences in the TC of the short circuit current and fill factor. We find a reasonable agreement between the simulated and experimental TCs, with the main difference being a ~0.02 %/K more negative TC in the open circuit voltage in the simulated values. This corresponds to only a 6-7% relative deviation from the experimental values, showing the validity of the PC1Dmod model.

INTRODUCTION

The conversion efficiency of a solar cell is usually determined under standard test conditions (STC), using a standard temperature of 25 °C and normal incidence, AM 1.5G irradiation with an intensity of 0.1 mW/cm^2. The operating conditions on the field may, however, deviate considerably from these standard conditions, with module temperatures routinely reaching temperatures of 60 °C or higher in warm climates. In order to correctly assess the actual power production of the solar modules in the field it is therefore important to know the performance under operating conditions. To relate the field efficiency (or other important solar cell parameters) to the value measured at STC, it is useful to define a *temperature coefficient* (TC), which is given as the relative change divided by the temperature interval (per ° C or K):

$$TC_X = \frac{100\%}{X_{STC}} \cdot \frac{X_{Top} - X_{STC}}{T_{op} - 25\,°C}, \tag{1}$$

where X is the parameter of interest and T_{op} is the operating cell temperature. For c-Si solar cells, the change in the IV parameters can usually safely be assumed to be linear in the relevant temperature range, meaning that the TCs can be expressed as a single value.

SiliconPV 2018, The 8th International Conference on Crystalline Silicon Photovoltaics
AIP Conf. Proc. 1999, 020010-1–020010-6; https://doi.org/10.1063/1.5049249
Published by AIP Publishing. 978-0-7354-1715-1/$30.00

One promising way of reducing the cost and energy requirement of Si production for solar cells is to use chemical purification steps such as slag treatment and leaching. This approach can give solar grade material quality without the need for the energy-demanding conversion to gaseous phase used in the Siemens process. The use of the metallurgical route results in the presence of both phosphorus and boron dopants in the feedstock, and the final material is therefore compensated. Additional boron and gallium dopants are normally introduced to obtain the target resistivity profile in the cast. In this work we have studied such wafers and solar cells based on Elkem Solar Silicon (ESS®). The motivation for the interest in the TCs of ESS®-based cells arise from the fact that several recent studies have shown that solar cells produced from ESS® material have beneficial traits compared to poly-Si in high temperature conditions. A difference in power yield between similarly rated modules with cells made of ESS® and polysilicon of between 1% and 2% over a year has been shown [1,2], which is best explained by a better temperature coefficient in ESS® cells. This effect has also been found on cell level, and studies indicate that the benefit in TCs mostly happens in the wavelength region 800 – 1100 nm, suggesting that the effect is connected to differences in lifetime and/or mobility at elevated temperature[3]. In this paper we aim to initiate a quantitative investigation of the contributions of different relevant mechanisms on the temperature dependency of the compensated ESS®-based cells by performing temperature-dependent device simulations in combination with experimental input data.

EXPERIMENTAL DETAILS

Wafers and cells taken from three different high performance multicrystalline (HPMC) silicon ingots have been investigated. Two ingots with target resistivities of 0.5 and 1.3 Ω-cm were produced using gallium co-doped ESS®, using a blend of 70% Elkem Solar Silicon and 30% polysilicon. Each dopant profile has been engineered to be as flat as possible by adding a combination of B and Ga (co-doping) in addition to the B and P dopants already present in the compensated silicon feedstock. In addition, a non-compensated ingot with a target resistivity of 1.3 Ω-cm, made with a blend of polysilicon and fluidized bed reactor (FBR) silicon feedstock, was cast as a reference. More information on the dopant profiles are given in Ref. [4].

Al-BSF-type solar cells were processed by ISC Konstanz using wafers taken at different heights of the three ingots and IV measurements were performed under 1 Sun simulated AM1.5G illumination at different temperatures to determine the experimental temperature coefficient of the IV parameters. Neighboring wafers were processed with phosphorous diffusion gettering and hydrogen passivation from PECVD a-SiNx:H coating and subsequent contact firing before etching and passivation in order to obtain lifetime data as similar as possible to that of the solar cells. Temperature dependent PL lifetime images were acquired using a LISR1 PL imaging setup from BTi in combination with a hotplate. The lifetime images were calibrated by temperature-dependent QSSPC measured automatically during cooling from ~120 to 25 °C using a Sinton WCT-120 TS setup in transient mode, following the procedure described in Ref. [5]. Dopant concentrations as a function of height in the ingots were determined using a combination of experimental resistivity data, simulations and the Scheil equation and used as input to the simulations at each height.

SIMULATION METHOD

Traditionally, device simulations of c-Si solar cells have been performed at 300 K, and not all the commonly used physical models and parameters are intended for use at other temperatures. In the recent years, the popular device simulation tool PC1D [6] has been updated with Fermi-Dirac statistics and several advanced models for various material properties of c-Si, several of which also includes temperature dependency in the relevant temperature range for solar cell operation[7–9]. One further complication for this work arises from the fact that the ESS® material is compensation doped, which also influences it's electrical and optical properties to a small degree. In this paper we attempt to use PC1Dmod6.2 to perform simulation of TCs of Al-BSF Si solar cells, using a selection of existing physical models and a few further alterations.

The most important effect of temperature of c-Si solar cells is the change in the intrinsic carrier density $n_{i,0}$, which again is determined by the intrinsic band gap energy $E_{g,0}$ and the effective density of states in the valence- and conduction band N_c and N_v:

$$n_{i,0} = \sqrt{N_c N_v} \exp\left(-\frac{E_{g,0}}{2k_B T}\right). \quad (2)$$

Because $n_{i,0}$ is so important for the determination of minority carrier concentrations, and thus the recombination properties of the solar cell, PC1Dmod uses a well-accepted model for $n_{i,0}(T)$ directly instead of basing $n_{i,0}(T)$ on

other parameterizations of N_c, N_v and $E_{g,0}$. $n_{i,0}(T)$ is then given by the parameterization by Sproul and Green's[10], which has been linearly scaled to match the commonly accepted value of 9.65×10^9 cm^{-3} at 300 K as reported by Altermatt et al.[11] (for a full description of the band structure parameters in PC1Dmod, see refs. [7,8]). In addition, we utilize the, doping- and injection-dependent band gap narrowing (BGN) model of Schenk [12] and mobility model of Schindler et al.[13] which includes contributions from the increased scattering term in compensation doped material. Furthermore, a small modification to the existing model for incomplete ionization of dopants[14] have been made in order to account for the simultaneous presence of P, B and Ga dopants in the material. The model for the temperature-dependence of the band gap E_g used in PC1Dmod[15] only influences the electrical band gap. The increased absorption coefficient caused by lowering of the optical band gap at higher temperatures has been accounted for by modifying the external file used to define the absorption coefficient, based on the data in ref. [16]. The temperature dependent lifetime images were used as input to the 1D model by performing a harmonic average over the image. Other cell parameters were taken from experimental input (dopant profile, J_{0e}, reflectance, contact shading etc). The rear side surface recombination velocity (SRV) in the PC1Dmod model was used as a free parameter and scaled linearly with the majority carrier equilibrium density p_0 in order to obtain a good match with the experimental data.

RESULTS AND DISCUSSION

One example of the temperature dependent lifetime images used as input to the simulations of TC's is shown in Fig. 1. Note that the lifetime in the investigated wafers generally increases at higher temperatures. A rather high temperature of 100 °C is used as comparison here in order to improve the visual contrast, whereas images acquired at 60 °C were used in the simulations. Fig. 1c) also shows the TC map of the carrier lifetime, illustrating that the lower-lifetime regions typically show a larger improvement when the temperature is increased, resulting in less contrast in the image at higher temperatures.

The experimental and simulated values for the four main IV parameters V_{oc}, J_{sc}, FF and conversion efficiency are given in Fig. 2. We observe that the 0.5 Ωcm ingot gives higher V_{oc} and a lower J_{sc} as expected from the higher dopant concentrations, and this is also reproduced in the simulations. A decreasing trend is observed in both V_{oc} and J_{sc} towards the top of all the three investigated ingots. We believe this to be mainly caused by a reduction in the harmonic average lifetime because of dislocation cluster growth towards the top of the ingot during casting. An increased dopant density towards the dop due to segregation was also found to be a contributing factor, particularly for the 0.5 Ωcm ingot. This observed dependence on ingot height is especially pronounced in the J_{sc} of the 0.5 Ωcm ingot. The same general trend is also observed in the simulations, but to a lesser extent, indicating that the simulation model does still not fully account for the influence of changes in lifetime and resistivity along the ingot height. One possible reason for this discrepancy might be that the harmonically averaged lifetime values does not describe the effect of dislocation clusters towards the top of this ingot correctly, and a more complete analysis based on local IV characteristics might be necessary in similar studies in the future.

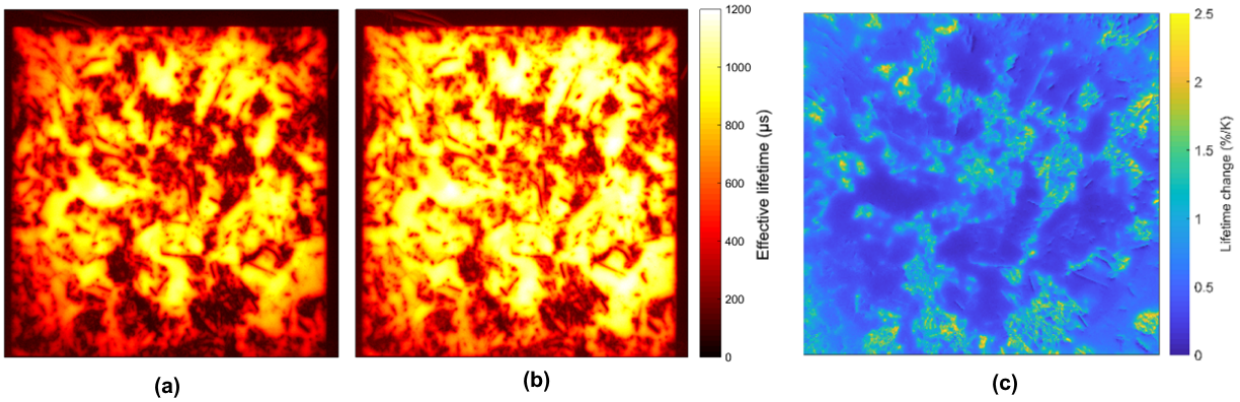

FIGURE 1. PL lifetime image in µs for a HPMC-Si wafer taken from the top part of the ESS® 1.3 Ωcm ingot, acquired at a) 25 °C and b) 100 °C. The map of the temperature coefficient of the carrier lifetime (relative lifetime change in % per K) is shown in (c).

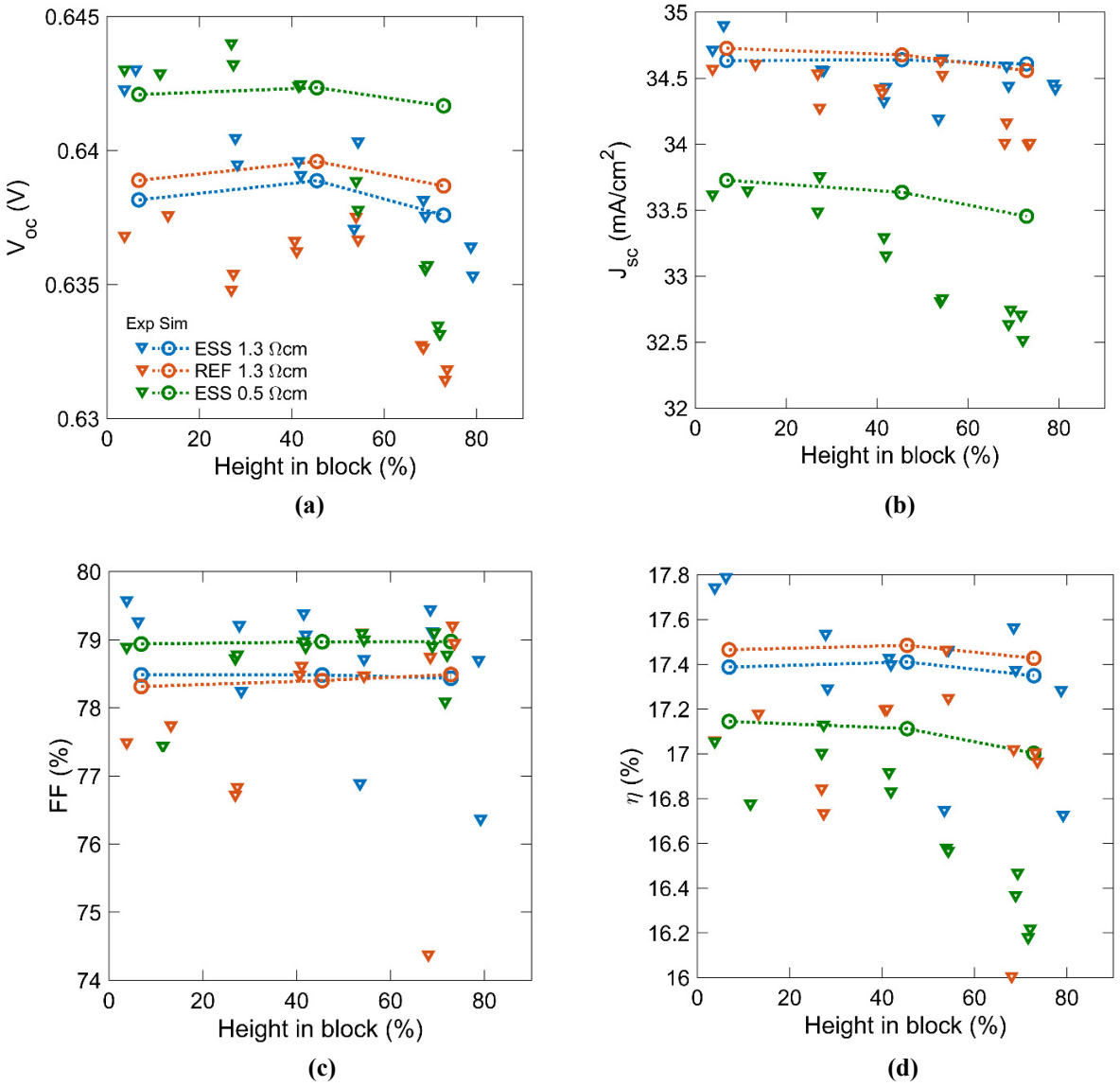

FIGURE 2. Values for the four main IV parameters: a) open circuit voltage, b) short circuit current, c) fill factor, and d) conversion efficiency as a function of block height for the three different blocks investigated in this work. Experimental values (triangles) are compared to PC1Dmod simulations (circles).

Fig. 3 shows a comparison of the experimental and simulated temperature coefficient of the four IV parameters at different ingot heights for each of the three ingots. We find a very good agreement in the absolute values for the TC_{Jsc} and TC_{FF} values, whereas the simulation predicts somewhat too large negative values for TC_{Voc}, which then naturally also causes a difference between the simulated and experimental values for TC_{η}. The offset is, however, only approximately 0.02 %/K, resulting in a ~6-7 % relative deviation from the experimental values. This discrepancy might be caused by an incomplete description of the involved physical properties of the cells in the models implemented in PC1Dmod, or by a systematic experimental error in the measured values. Both the simulated and experimental results are within the range of previously reported values for combinations of TC_{Voc} and the V_{oc} itself. Note that the model is able to reproduce the improved TC_{Jsc} in the cells made with higher base doping (0.5 Ωcm material) in addition to the increasing trend with ingot height observed for these cells. We therefore regard this result as a good validation that the simulation model works as intended and can be used for predictions and quantitative analysis of c-Si solar cells also at temperatures higher than 300 K.

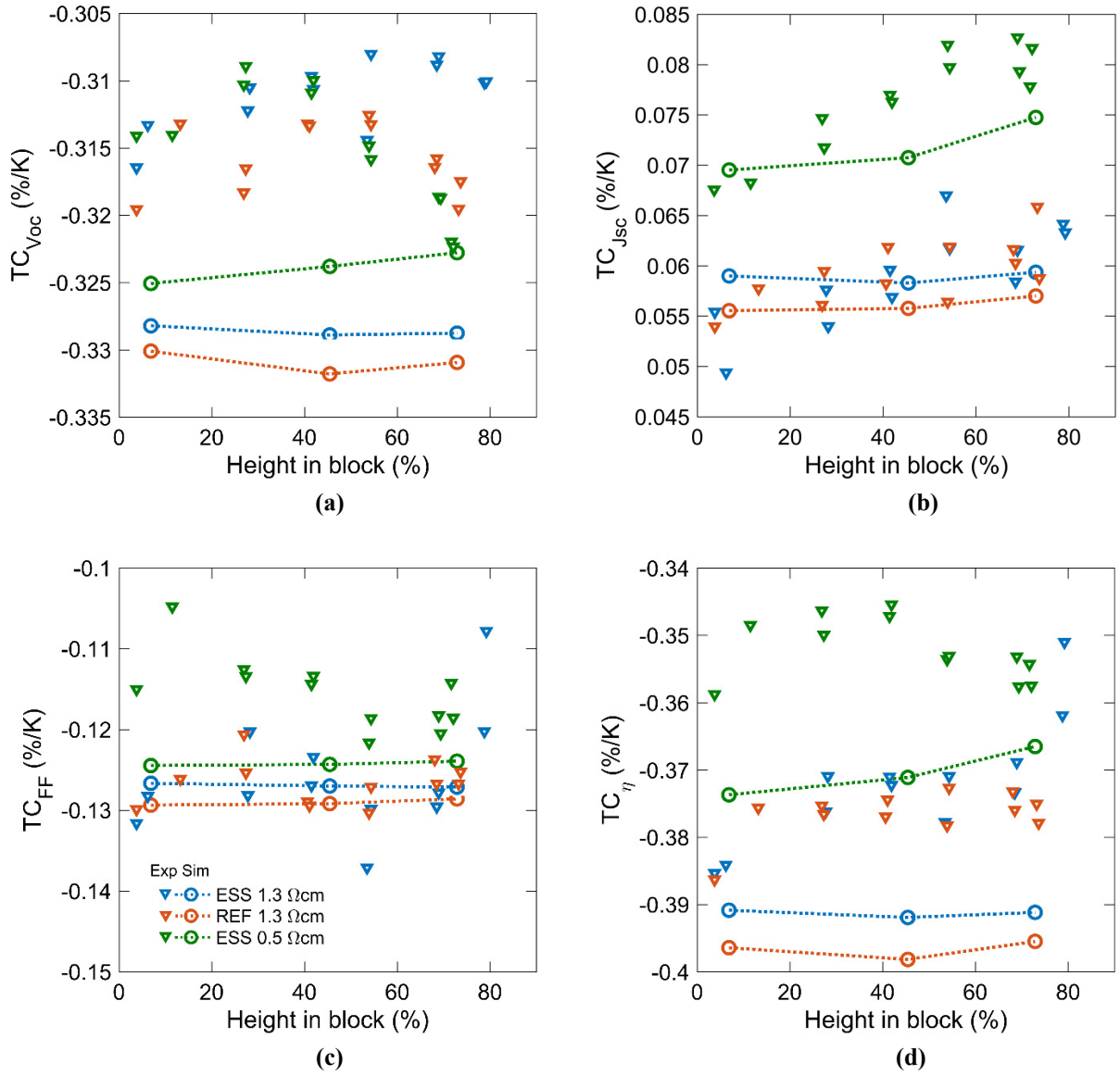

FIGURE 3. Temperature coefficients in the four main IV parameters: a) open circuit voltage, b) short circuit current, c) fill factor, and d) conversion efficiency as a function of block height for the three different blocks investigated in this work. Experimental values (triangles) are compared to PC1Dmod simulations (circles).

CONCLUSION AND FURTHER WORK

By using a collection of advanced models for c-Si implemented in PC1Dmod6.2 we have verified that the program is able to predict the temperature dependent behavior of Al-BSF c-Si solar cells, after comparison with experimental IV measurements. The harmonic average of temperature dependent lifetime images and calculated dopant concentrations at each wafer position were used as input to the simulations, and were needed to obtain a good agreement with measurements. We observe a qualitative difference between the 1.3 Ωcm ingots and the 0.5 Ωcm ingot in both the experiments and the simulations, which is due to differences in both resistivity and material quality. For the 1.3 Ωcm ingots higher temperature coefficients were predicted in the compensated material than in the non-compensated reference based on previous results on the subject. We do not observe this in the measurements in this work, which might be explained by a higher material quality in the 1.3 Ωcm ingots and limited efficiency of the cells,

so that the cells are not mainly limited by the bulk diffusion length. A similar TC for the two 1.3 3 Ωcm ingots is also found in the simulations.

After verifying the model in this work, it will be used to perform a sensitivity analysis of the different factors influencing the temperature coefficient of c-Si solar cells, hopefully being able to determine the root causes for the observed relative improvements of the compensated ESS® material under elevated temperature in the field.

ACKNOWLEDGMENTS

The authors want to thank the team at ISC Konstanz for help with solar cell processing. Funding for this work was provided through the EnergiX programme of the Norwegian Research Council, project number 256271 - Performance and Reliability IN Compensated Elkem Solar Silicon.

REFERENCES

1. J.O. Odden, T.C. Lommasson, M. Tayyib, J. Vedde, T. Buseth, K. Friestad, H. Date, and R. Tronstad, Sol. Energy Mater. Sol. Cells **130**, 673 (2014).
2. M. Tayyib et al., Proceedings of the 40th IEEE Photovolt. Spec. Conf. PVSC (2014) pp. 3230-3233.
3. R. Søndenå, C. Berthod, J.O. Odden, A.-K. Søiland, M.S. Wiig, and E. Stensrud Marstein, Energy Procedia 77, 639 (2015).
4. R. Søndenå, H. Haug, A. Song, E. Hsueh, and J.O. Odden, in AIP Conf. Proc. (to Be Publ. (2018).
5. H. Haug, R. Søndenå, M.S. Wiig, and E.S. Marstein, Energy Procedia **124**, 47 (2017).
6. D.A. Clugston and P.A. Basore, Proceedings o the 26th IEEE Photovolt. Spec. Conf. PVSC (1997) pp. 207-210
7. H. Haug, A. Kimmerle, J. Greulich, A. Wolf, and E. Stensrud Marstein, Sol. Energy Mater. Sol. Cells 131, 30 (2014).
8. H. Haug, J. Greulich, A. Kimmerle, and E.S. Marstein, Sol. Energy Mater. Sol. Cells **142**, 47-53 (2015).
9. H. Haug and J. Greulich, Energy Procedia **92**, 60-68 (2016).
10. A.B. Sproul and M.A. Green, J. Appl. Phys. **73**, 1214 (1993).
11. P.P. Altermatt, A. Schenk, F. Geelhaar, and G. Heiser, J. Appl. Phys. **93**, 1598 (2003).
12. A. Schenk, J. Appl. Phys. **84**, 3684 (1998).
13. F. Schindler, M. Forster, J. Broisch, J. Schön, J. Giesecke, S. Rein, W. Warta, and M.C. Schubert, Sol. Energy Mater. Sol. Cells **131**, 92-99 (2014).
14. P.P. Altermatt, A. Schenk, B. Schmithüsen, and G. Heiser, J. Appl. Phys. **100**, 113715 (2006).
15. M.A. Green, J. Appl. Phys. **67**, 2944 (1990).
16. H.T. Nguyen, F.E. Rougieux, B. Mitchell, and D. Macdonald, J. Appl. Phys. **115**, 1 (2014).